AIP | Applied Physics Letters

Fast imaging with alternative signal for dynamic atomic force microscopy

Chibum Lee and Srinivasa M. Salapaka

Citation: Appl. Phys. Lett. **97**, 133101 (2010); doi: 10.1063/1.3495987
View online: http://dx.doi.org/10.1063/1.3495987
View Table of Contents: http://apl.aip.org/resource/1/APPLAB/v97/i13
Published by the AIP Publishing LLC.

Fast imaging with alternative signal for dynamic atomic force microscopy

Chibum Lee and Srinivasa M. Salapaka[a)]
Department of Mechanical Science and Engineering, University of Illinois at Urbana-Champaign, Illinois 61801, USA

(Received 29 June 2010; accepted 7 September 2010; published online 27 September 2010)

In this paper, a method for imaging in amplitude-modulation atomic force microscopy is developed which enables accurate sample-profile imaging even at high scanning speeds where existing methods that use the actuator input signal fail. The central concept is to use a model of the vertical positioning actuator to compensate for the artifacts introduced due to its compliance in high scanning frequencies. We provide experiments that compare sample-profile estimates from our method with the existing methods and demonstrate significant improvement (by 70%) in the estimation bandwidth. The proposed design allows for specifying a trade-off between the sample-profile estimation error and estimation bandwidth. © *2010 American Institute of Physics*. [doi:10.1063/1.3495987]

Amplitude-modulation atomic force microscopy (AM-AFM) (Ref. 1) is the most common mode used in AFM, especially for scanning biological surfaces, since the cantilever tip comes in contact only intermittently and gently with the sample without any shear forces and therefore does not damage the sample. In this mode, a microcantilever is made to oscillate sinusoidally over a sample-surface, and the changes in the amplitude of the cantilever tip oscillations due to its interaction with the topographic features on sample are used to derive the sample profile. In a typical operation, the cantilever-oscillation amplitude is maintained at a constant value by using a piezoactuator to move the sample vertically in order to compensate for the features on the sample surface. The voltage input given to the actuator that compensates for the sample features provides a measure of the sample profile. The main disadvantage of this mode is that imaging bandwidth is limited since at high scanning frequencies, the piezoactuator is not rigid but is compliant. At these scanning frequencies, the voltage input to the actuator is indicative of *both* the deformation of the piezoactuator and the sample features, and therefore is an inaccurate measure of sample profile alone. Therefore, in typical AM-AFM, the imaging bandwidth is limited by the bandwidth of the piezoactuator. The main idea in this paper is to derive a measurable signal that exploits a dynamic model of the piezoactuator to give an accurate measure of the sample profile. Conceptually, it utilizes both the voltage input to the piezoactuator and the cantilever deflection signal, and therefore is not limited by the bandwidth of the piezoactuator.

A model of dynamic AFM is described in Fig. 1, where device components are represented by transfer functions.[2] Transfer functions represent dynamics of components about a nominal operating point. The cantilever dynamics $\mathcal{F}$ which includes the tip-sample interaction force F_{ts}, the external excitation force $g(t)$ of dither piezo, and the thermal noise η is given by

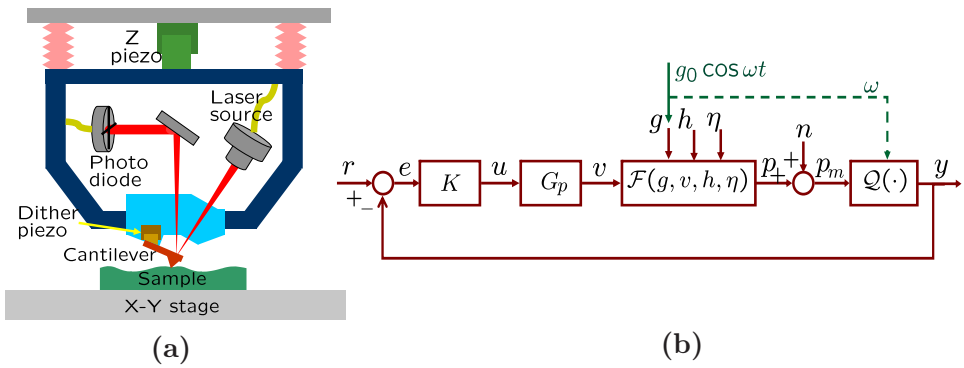

FIG. 1. (Color online) (a) A schematic of imaging system of dynamic AFM. The cantilever is attached to a vertical positioner. The oscillation of the cantilever is sensed, and a feedback controller moves the positioner to maintain a constant amplitude of cantilever oscillation in AM-AFM. (b) The block diagram of the AFM. K, G_p, $\mathcal{F}$, and $\mathcal{Q}$ represent the controller, the vertical piezopositioner, the cantilever dynamics model, and the lock-in amplifier or rms-to-dc converter, respectively. In AM-AFM, the dither piezo is oscillated at a frequency ω close to the cantilever natural frequency. The controller, K, is to regulate the difference, e, between an amplitude, y, of the deflection signal, p, and the set point r to zero to compensate the effects of the sample topography h. The deflection, p, is due to the forcing of the nonlinear dynamic model $\mathcal{F}$, the dither piezoexcitation g, the thermal noise η, and the tip-sample interaction force F_{ts} that depends on the sample-position v by vertical piezoactuator and the sample height h. The deflection measurements p_m are corrupted by sensor noise, that is, $p_m=p+n$.

[a)]Electronic mail: salapaka@illinois.edu.

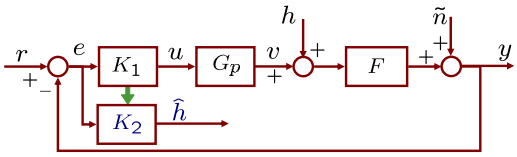

FIG. 2. (Color online) Block diagram for the proposed method of sample-topography estimation. $\hat{h}$ is a designed estimate signal. The multi-input cantilever dynamics model $\mathcal{F}(g,v,h,\eta)$ and lock-in amplifier $\mathcal{Q}(\cdot)$ in Fig. 1 is approximated by the single input model F.

$$\ddot{p} + \frac{\omega_0}{Q}\dot{p} + \omega_0^2 p = \frac{1}{m}F_{ts}(p-h-v) + g(t) + \eta. \tag{1}$$

In typical AM-AFM imaging, the control signal u (the voltage input to the actuator) is used to obtain an estimate of the sample topography h. The rationale is that if the thermal noise η and sensor noise n are neglected, the amplitude of deflection p is maintained at a constant value when (averaged) interaction force F_{ts} in one oscillation is approximately constant which in turn implies $-h-v=0$. Since G_p is approximately a constant $G_p(0)$ at low frequencies, the control signal u gives a measure proportional to $h=-v\approx -G_p(0)u$ for low speed scans (or smooth samples). However, this signal yields distorted images for high speed scans (or rough samples) since G_p is not constant and u is not proportional to sample position v at high frequencies. Thus, for good imaging, the controller K is required to give an accurate estimate for the sample topography h as well as to regulate the amplitude of deflection p to compensate the effects of the sample topography, which is not easy to achieve simultaneously.

In the proposed method shown in Fig. 2, an alternative signal $\hat{h}$ for estimating the topography is generated by designing a separate estimator transfer function K_2 that fully utilizes the information in the system. (A similar signal was used for contact mode AFM (Ref. 3) but the derivation of the signal was based on a different approach.) The best estimate $\hat{h}$ of sample topography minimizes the estimation error $\tilde{h}=h-\hat{h}$. It is assumed that the set-point regulation controller K_1 is given or fixed. Here, F represents the map whose output is the amplitude y of the deflection signal when its input is the sum of the sample-topography h and the piezoactuation signal v. The uncertainties in using F, the effect of the thermal noise η, and the sensor noise n are represented by $\tilde{n}$. Based on our identification experiments using constant dither excitation $g(t)=g_0\cos\omega t$, the cantilever dynamics F is found to be nearly linear at low frequencies. When a cantilever of natural frequency $f_n\approx 70$ kHz is used, the frequency response ≤ 2 kHz is almost linear, which also implies $\tilde{n}$ is dominant in high frequencies >2 kHz.

If we assume that the given controller K_1 and the vertical piezomodel G_p are linear, the input u is given by

$$u = SK_1(r-\tilde{n}) - SK_1Fh, \tag{2}$$

where the sensitivity transfer function is written as $S=(1+K_1FG_p)^{-1}$. The transfer function from the sample profile h to the control signal u is given by $T_{uh}=SK_1F=K_1F/(1+G_pK_1F)$ and approximated by $T_{uh}\approx 1/G_p$ since typically K_1 is large at low frequencies for good amplitude regulation. This fortifies the conventional estimate $|G_p(0)|u$ of the sample topography h. However, K_1 cannot be designed to be large at high frequencies (since it can make the closed-loop unstable or induce chattering), and G_p is not a constant at high frequencies, the transfer function T_{uh} is not a constant. Therefore, the conventional estimate $|G_p(0)|u$ gives low fidelity images during fast scanning. A simple solution to this problem, that ensures good imaging, is to use a slow lateral scanning speed which will make h a low frequency signal with the moderate controller K_1 (Note that the temporal frequency content of h depends on the spatial frequency content of the sample, i.e., how rough the sample is, and the scanning speed of the X-Y positioners, i.e., how fast the sample is scanned). However, this solution comes by sacrificing bandwidth, which is not tenable in many applications.

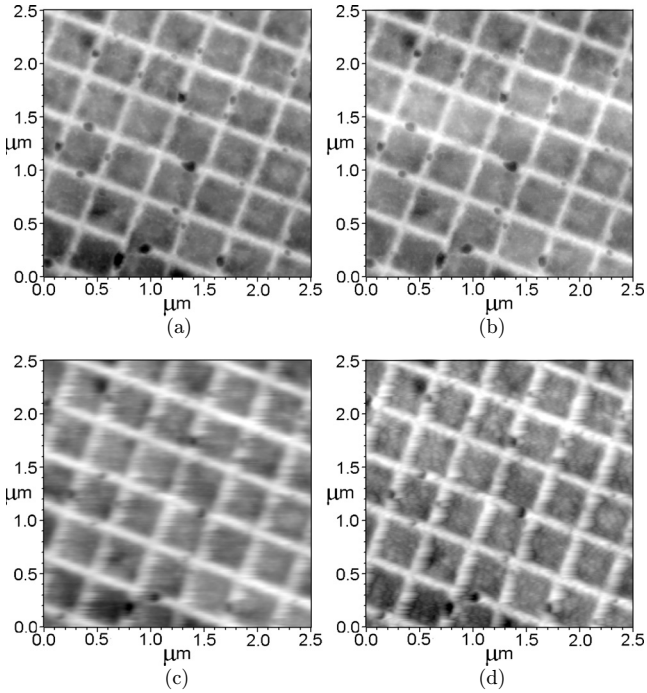

FIG. 3. Comparison of 2D image of conventional (left) and proposed (right) estimation: [(a) and (b)] scan rate of 5 μm/s. [(c) and (d)] scan rate of 100 μm/s.

In the proposed method, we use a separate estimator K_2 and design a signal $\hat{h}$ that leads to an increase in the imaging bandwidth for a prespecified controller. In this case, the estimate signal $\hat{h}$ and the estimation error $\tilde{h}$ are given by

$$\hat{h} = K_2S(r-\tilde{n}) - K_2FSh, \tag{3}$$

$$\tilde{h} = -K_2S(r-\tilde{n}) + (1+K_2FS)h, \tag{4}$$

and therefore the transfer function from the sample profile h to the designed estimation signal $\hat{h}$ is given by $T_{\hat{h}h}=-K_2FS=-K_2F/(1+G_pK_1F)$. From Eq. (4), it is evident that the sample profile estimation design needs to consider effects of the sample profile h as well as the noise $\tilde{n}$. The estimator design $K_2=-S^{-1}F^{-1}=(1+K_1FG_p)F^{-1}$ annuls the effect of sample topography h; however the effect of noise $\tilde{n}$ in sample-profile estimation error $\tilde{h}$ is then given by $K_2S\tilde{n}=F^{-1}\tilde{n}$. We introduce a weight function W_h that allows us to specify a trade-off between the effects of $\tilde{n}$ and h, whereby the estimator design is given by

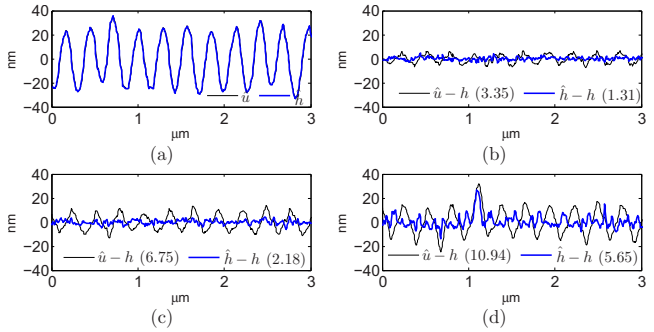

FIG. 4. (Color online) Comparison of the conventional $|G_p(0)|u$ and the designed estimate signal $\hat{h}$: (a) $\hat{u}$ (thin, black) and the $\hat{h}$ (thick, blue) in scan rate of 4 μm/s. [(b)–(d)] $|G_p(0)|u-h$ (thin, black) and $\hat{h}-h$ (thick, blue) in scan rate of 10 μm/s (b), 20 μm/s (c), and 40 μm/s (d). (rms errors are shown.)

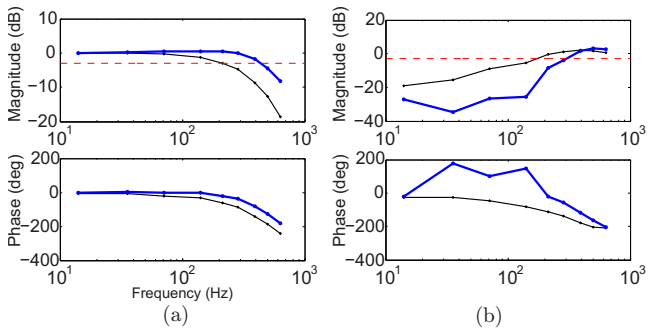

FIG. 5. (Color online) (a) Experimentally obtained transfer function from the sample height h to the conventional height estimate $|G_p(0)|u$ (thin, black) and to the designed height estimate $\hat{h}$ (thick, blue) (b) transfer function from the sample height h to the conventional height estimation error $h-|G_p(0)|u$ (thin, black) and to the designed height estimation error $h-\hat{h}$ (thick, blue).

$$K_2 = -S^{-1}F^{-1}W_h, \tag{5}$$

and the corresponding estimation error is given by $\tilde{h}=-F^{-1}W_h(r-\tilde{n})+(1-W_h)h$. The choice of low pass filter for the weight function W_h makes the effect of noise $F^{-1}W_h\tilde{n}$ small since the noise $\tilde{n}$ is primarily a high frequency signal. In the experimental demonstration presented in this paper, since $\tilde{n}$ is dominant in frequencies >2 kHz, W_h is chosen as a low pass filter with 2 kHz bandwidth.

The proposed method separates the goals of force regulation and sample-topography estimation by designing two signals—u for force regulation and $\tilde{h}$ for estimating the sample topography h. In particular, in this method, the design of controller K_1 for regulation can be made without any consideration toward estimation of sample topography and the estimation bandwidth is not limited by the regulation bandwidth. That is, in contrast to the existing methods, this separation of goals in the proposed allows the sample-profile estimation bandwidth to extend beyond the disturbance rejection bandwidth achieved by the controller K_1 designed for the force regulation. Also, this increased bandwidth is achieved without any instability or chattering issues, where the sensitivity of the regulation and topography estimation to various model inaccuracies are solely determined by the regulation controller K_1.

To verify the proposed method, a two-dimensional (2D) calibration grating consisting of ridges that are 31 nm high and spaced 463 nm apart was imaged. Figure 3 shows 2D images constructed from the conventional estimation $|G_p(0)|u$ in the left column and from our estimate signal $\hat{h}$ in the right column. Note that the images in the left and right columns are obtained simultaneously during the same scan. The difference is not noticeable in slow scan (5 μm/s) images in Figs. 3(a) and 3(b). However, fast scan (100 μm/s) images show that the image obtained from the proposed method in Fig. 3(d) has greater clarity than the image in Fig. 3(c) and closer to the slow scan images in Figs. 3(a) and 3(b). To compare the estimation performance between the conventional estimate and the proposed estimate signal, a one-dimensional calibration sample with ridges of height of 50 nm spaced 278 nm apart was imaged. Figure 4 compares the conventional estimate signal $|G_p(0)|u$ and the proposed estimate signal $\hat{h}$. For very slow scan in Fig. 4(a), both signals are almost identical, so the average of them is used as the reference signal h. Figures 4(b)–4(d) show that the conventional-design estimate error $|G_p(0)|u-h$ are significantly worse (94%–210%) than the proposed-design estimate errors $\tilde{h}-h$ at different scanning speeds. The transfer functions from the sample height h to the conventional estimate $|G_p(0)|u$ and proposed estimate $\tilde{h}$ (obtained from the experimental data) in Fig. 5(a) show that the proposed design gives a better estimate of the sample topography h over a larger bandwidth. This conclusion is made even more evident in Fig. 5(b) where the conventional estimation and the proposed estimation bandwidths are shown to be 177 Hz and 301 Hz, respectively, where imaging bandwidth is defined as the frequency at which the magnitude of estimation reaches $1/\sqrt{2}$. In this figure, it is assumed that the input is the same as the calculated reference in Fig. 4(a) which has a maximum rms error of 2.3 nm. More detail on analysis and discussion can be found in the Ph.D dissertation of the first author.[4]

The authors were supported by NSF Grant Nos. CMMI 0800863 and ECCS 0925701.

[1]R. García and R. Pérez, Surf. Sci. Rep. **47**, 197 (2002).
[2]J. Bechhoefer, Rev. Mod. Phys. **77**, 783 (2005).
[3]S. Salapaka, T. De, and A. Sebastian, Appl. Phys. Lett. **87**, 053112 (2005).
[4]C. Lee, Ph.D. thesis, University of Illinois at Urbana-Champaign, 2010.